Organometallics **1991,** *10,* 963–970

Chemistry of *C*-Trimethylsilyl-Substituted Main-Group Heterocarboranes. 8. Synthesis of *closo*-Gallacarboranes and Their Reactivity toward a Bis(bidentate) Lewis Base, 2,2′-Bipyrimidine: Crystal Structures of *closo*-$1\text{-}(t\text{-}C_4H_9)\text{-}1\text{-}Ga\text{-}2,3\text{-}(SiMe_3)_2\text{-}2,3\text{-}C_2B_4H_4$ and $1,1'\text{-}(2,2'\text{-}C_8H_6N_4)[1\text{-}(t\text{-}C_4H_9)\text{-}1\text{-}Ga\text{-}2,3\text{-}(SiMe_3)_2\text{-}2,3\text{-}C_2B_4H_4]_2$

Narayan S. Hosmane,* Kai-Juan Lu, Hongming Zhang, and Lei Jia

Department of Chemistry, Southern Methodist University, Dallas, Texas 75275

Alan H. Cowley* and Miguel A. Mardones

Department of Chemistry, University of Texas at Austin, Austin, Texas 78712

Received July 31, 1990

The reaction of $[Ga(t\text{-}C_4H_9)Cl_2]_2$ with the *nido*-carborane dianionic double salts $Na^+Li^+[2\text{-}(SiMe_3)\text{-}3\text{-}(R)\text{-}2,3\text{-}C_2B_4H_4]^{2-}$ (R = $SiMe_3$, Me, H) in a molar ratio of 1:2 in THF produced *closo*-$1\text{-}(t\text{-}C_4H_9)\text{-}1\text{-}Ga\text{-}2,3\text{-}(SiMe_3)_2\text{-}2,3\text{-}C_2B_4H_4$ (I), *closo*-$1\text{-}(t\text{-}C_4H_9)\text{-}1\text{-}Ga\text{-}2\text{-}(SiMe_3)\text{-}3\text{-}(Me)\text{-}2,3\text{-}C_2B_4H_4$ (II), and *closo*-$1\text{-}(t\text{-}C_4H_9)\text{-}1\text{-}Ga\text{-}2\text{-}(SiMe_3)\text{-}2,3\text{-}C_2B_4H_5$ (III) as moderately air-sensitive colorless oily liquids, in 71, 83, and 62% yields, respectively. In addition, the corresponding neutral *nido*-carborane precursor $2\text{-}(SiMe_3)\text{-}3\text{-}(R)\text{-}2,3\text{-}C_2B_4H_6$ was produced in yields ranging from 14 to 36%. The *closo*-gallacarboranes I–III were characterized on the basis of ^1H, ^{11}B, and ^{13}C pulse Fourier transform NMR, IR, and mass spectroscopy. The low-temperature, single-crystal X-ray analysis of I shows that the gallacarborane has a closo geometry in which the gallium atom occupies an apical vertex in a distorted pentagonal bipyramid. The gallium-bound *tert*-butyl group makes a pronounced tilt toward the cage carbons above the C_2B_3 face with angles of about 21 and 24° to the axis that bisects the apical boron and gallium and the axis that bisects the apical gallium and the centroid of the C_2B_3 face, respectively. The *closo*-gallacarborane I crystallized in the triclinic space group $P\bar{1}$ with $a = 9.160$ (2) Å, $b = 9.763$ (3) Å, $c = 12.961$ (4) Å, $\alpha = 96.84$ (2)°, $\beta = 106.56$ (2)°, $\gamma = 111.20$ (2)°, $V = 1003.3$ (5) Å^3, and $Z = 2$. Full-matrix least-squares refinements of I converged at $R = 0.047$ and $R_w = 0.063$. The instantaneous reaction between *closo*-gallacarboranes and 2,2′-bipyrimidine produced the donor–acceptor complexes $1,1'\text{-}(2,2'\text{-}C_8H_6N_4)[1\text{-}(t\text{-}C_4H_9)\text{-}1\text{-}Ga\text{-}2,3\text{-}(SiMe_3)_2\text{-}2,3\text{-}C_2B_4H_4]_2$ (IV), $1,1'\text{-}(2,2'\text{-}C_8H_6N_4)[1\text{-}(t\text{-}C_4H_9)\text{-}1\text{-}Ga\text{-}2\text{-}(SiMe_3)\text{-}3\text{-}(Me)\text{-}2,3\text{-}C_2B_4H_4]_2$ (V), and $1,1'\text{-}(2,2'\text{-}C_8H_6N_4)[1\text{-}(t\text{-}C_4H_9)\text{-}1\text{-}Ga\text{-}2\text{-}(SiMe_3)\text{-}2,3\text{-}C_2B_4H_5]_2$ (VI) in 74–86% yields. The complexes IV–VI were characterized by ^1H, ^{11}B, and ^{13}C NMR, IR, and mass spectroscopy. A single-crystal X-ray analysis was also performed on complex IV. The structure shows that the 2,2′-bipyrimidine base bridges the two gallacarboranes with a center of inversion between the carbons that link the two pyrimidine bases. The apical gallium in each cage is slipped severely from the centroidal position above the C_2B_3 face in such a way that it could be considered as η^1 bonded to the unique boron. Consequently, the Ga-bound *tert*-butyl group is significantly more tilted from the Ga–C_2B_3 centroid axis toward the cage carbons by about 56.3° than in the precursor, despite the steric hindrance of the bulky trimethylsilyl groups on the cage carbons. Complex IV crystallized in the monoclinic space group $C2/c$ with $a = 24.732$ (10) Å, $b = 14.190$ (4) Å, $c = 15.797$ (5) Å, $\beta = 117.97$ (3)°, $V = 4896$ (2) Å^3, and $Z = 4$. Full-matrix least-squares refinement of IV converged at $R = 0.051$ and $R_w = 0.061$.

Introduction

The aluminacarboranes constitute the best known group 13 heterocarboranes.[1-9] Icosahedral *commo-* and *closo*-aluminacarboranes based on C_2B_9 and C_2B_8 systems have been well characterized both structurally and spectroscopically. Moreover, reactivity studies have revealed that such compounds can function as useful dicarbollyl transfer agents when treated with main-group halides.[10] This general area has been reviewed.[11,12] Most recently, the structure of a triethylphosphine adduct of a *closo*-aluminacarborane of the C_2B_9 system has been reported.[13] Interestingly, aluminacarboranes based on C_2B_4 fragments have proved to be elusive. In fact, the only examples of such species are a bridged derivative[14] and seven-vertex *nido-* and *commo*-aluminacarboranes[15] in which the group

---

(1) Young, D. A. T.; Wiersema, R. J.; Hawthorne, M. F. *J. Am. Chem. Soc.* **1971,** *93,* 5687.

(2) (a) Young, D. A. T.; Willey, G. R.; Hawthorne, M. F.; Churchill, M. R.; Reis, A. H., Jr. *J. Am. Chem. Soc.* **1970,** *92,* 6663. (b) Churchill, M. R.; Reis, A. H., Jr. *J. Chem. Soc., Dalton Trans.* **1972,** 1317.

(3) Rees, W. S., Jr.; Schubert, D. M.; Knobler, C. B.; Hawthorne, M. F. *J. Am. Chem. Soc.* **1986,** *108,* 5367.

(4) Bandman, M. A.; Knobler, C. B.; Hawthorne, M. F. *Inorg. Chem.* **1988,** *27,* 2399.

(5) Schubert, D. M.; Knobler, C. B.; Rees, W. S., Jr.; Hawthorne, M. F. *Organometallics* **1987,** *6,* 201.

(6) Schubert, D. M.; Knobler, C. B.; Rees, W. S., Jr.; Hawthorne, M. F. *Organometallics* **1987,** *6,* 203.

(7) Schubert, D. M.; Knobler, C. B.; Hawthorne, M. F. *Organometallics* **1987,** *6,* 1353.

(8) Schubert, D. M.; Rees, W. S., Jr.; Knobler, C. B.; Hawthorne, M. F. *Pure Appl. Chem.* **1987,** *59,* 869.

(9) Mikhailov, B. M.; Potapova, T. V. *Izv. Akad. Nauk, SSSR, Ser. Khim.* **1968,** *5,* 1153.

(10) Jutzi, P.; Galow, P. *J. Organomet. Chem.* **1987,** *319,* 139.

(11) Hosmane, N. S.; Maguire, J. A. Advances in Boron and the Boranes. In *Molecular Structure and Energetics*; Liebman, J. F., Greenberg, A., Williams, R. E., Eds.; VCH: New York, 1988; Vol. 5, Chapter 14, p 297.

(12) Hosmane, N. S.; Maguire, J. A. *Adv. Organomet. Chem.* **1990,** *30,* 99.

(13) Schubert, D. M.; Bandman, M. A.; Rees, W. S., Jr.; Knobler, C. B.; Lu, P.; Nam, W.; Hawthorne, M. F. *Organometallics* **1990,** *9,* 2046.

(14) Magee, C. P.; Sneddon, L. G.; Beer, D. C.; Grimes, R. N. *J. Organomet. Chem.* **1975,** *86,* 159.

(15) Beck, J. S.; Sneddon, L. G. *J. Am. Chem. Soc.* **1988,** *110,* 3467.

13 moiety is η^3 bonded to the carborane cage. No X-ray crystallographic data are available for these compounds.

Significantly less is known about the carborane derivatives of the heavier group 13 elements. To our knowledge, no indium carboranes have been structurally characterized and gallium derivatives are confined to *closo*-1-Me-1-Ga-2,3-$C_2B_4H_6$[16] and [*commo*-3,3'-Ga(3,1,2-$GaC_2B_9H_{11})_2]^-$.[17] No information is available regarding the coordination chemistry of the gallacarboranes. In the present paper we describe the preparation, characterization, and properties of *C*-trimethylsilyl-substituted *closo*-gallacarboranes and their 2,2'-bipyrimidine complexes. In addition, we report the X-ray crystal structures of *closo*-1-(*t*-C_4H_9)-1-Ga-2,3-$(SiMe_3)_2$-2,3-$C_2B_4H_4$ (I) and its donor–acceptor complex 1,1'-(2,2'-$C_8H_6N_4$)[1-(*t*-C_4H_9)-1-Ga-2,3-$(SiMe_3)_2$-2,3-$C_2B_4H_4]_2$ (IV).

Experimental Section

Materials. 2,3-Bis(trimethylsilyl)-2,3-dicarba-*nido*-hexaborane(8), 2-(trimethylsilyl)-3-methyl-2,3-dicarba-*nido*-hexaborane(8), and 2-(trimethylsilyl)-2,3-dicarba-*nido*-hexaborane(8) were prepared by the methods of Hosmane et al.[18-21] Solutions of the sodium salts of the *nido*-carborane monoanions [2-$(SiMe_3)$-3-(R)-2,3-$C_2B_4H_5]^-$ (R = $SiMe_3$, Me, H) in tetrahydrofuran (THF) were prepared by the method described elsewhere.[22] The dimer [Ga(*t*-$C_4H_9)Cl_2]_2$ was prepared and purified according to the literature method.[23] The purity of the gallium reagent was checked by IR and NMR spectroscopy and on the basis of the melting point. Prior to use, 2,2'-bipyrimidine (Lancaster Syntheses, Windham, NH) was sublimed in vacuo, and the purity was checked by IR, NMR, and melting point measurements. A 1.7 M solution of *tert*-butyllithium (*t*-BuLi) in *n*-pentane was obtained from Aldrich Chemical Co., Milwaukee, WI, and used as received. NaH (Aldrich) in a mineral oil dispersion was washed repeatedly with dry pentane. Benzene and THF were dried over $LiAlH_4$ and doubly distilled before use. All other solvents were dried over 4–8-Å molecular sieves (Davidson) and either saturated with dry argon or degassed before use.

Spectroscopic Procedures. Proton, boron-11, and carbon-13 pulse Fourier transform NMR spectra, at 200, 64.2, and 50.3 MHz, respectively, were recorded on an IBM-200 SY multinuclear NMR spectrometer. Infrared spectra were recorded on a Perkin-Elmer Model 283 infrared spectrometer and a Perkin-Elmer Model 1600 FT-IR spectrophotometer. Mass spectral determinations were performed by the Midwest Center for Mass Spectrometry, University of Nebraska–Lincoln, Lincoln, NE.

Synthetic Procedures. All experiments were carried out in Pyrex glass round-bottom flasks of 250-mL capacity, containing magnetic stirring bars and fitted with high-vacuum Teflon valves. Nonvolatile substances were manipulated in either a drybox or evacuable glovebags under an atmosphere of dry nitrogen. All known compounds among the products were identified by comparing their IR and ^1H NMR spectra with those of authentic samples.

Synthesis of *closo*-1-(*t*-C_4H_9)-1-Ga-2-$(SiMe_3)$-3-(R)-2,3-$C_2B_4H_4$ (R = Me_3Si, Me, H). In a procedure identical with that employed for the synthesis of *commo*-silabis(carborane) and *closo*-germacarboranes, described elsewhere,[24-26] 6.56 mL (0.714 g, 11.15 mmol), 5.82 mL (0.634 g, 9.90 mmol), or 6.03 mL (0.657 g, 10.25 mmol) of 1.7 M *t*-BuLi in pentane was slowly added to a THF (50 mL) solution of Na^+[2,3-$(SiMe_3)_2$-2,3-$C_2B_4H_5]^-$ (2.67 g, 11.15 mmol), Na^+[2-$(SiMe_3)$-3-(Me)-2,3-$C_2B_4H_5]^-$ (1.80 g, 9.90 mmol), or Na^+[2-$(SiMe_3)$-2,3-$C_2B_4H_6]^-$ (1.72 g, 10.25 mmol) in vacuo at −23 °C, and the resulting homogeneous solution of the lithium sodium carborane double salts Li^+Na^+[2-$(SiMe_3)$-3-(R)-2,3-$C_2B_4H_5]^{2-}$ (R = $SiMe_3$, Me, H) was stirred constantly at this temperature for 1 h. This solution was then cooled to −78 °C and the volatiles (presumably, 2-methylpropane and pentane) were quickly pumped off from the reaction flask. After it was warmed to −23 °C, the solution was poured slowly in vacuo onto the freshly prepared, anhydrous [Ga(*t*-$C_4H_9)Cl_2]_2$ (1.884 g, 4.76 mmol; 1.958 g, 4.95 mmol; 2.026 g, 5.124 mmol) at −23 °C, and the mixture was stirred constantly for 2 h. After removal of THF at this temperature via vacuum distillation for 2 h, the reaction flask containing an off-white residue was attached to a detachable high-vacuum U-trap that was immersed in a dry-ice/2-propanol bath. With fractional distillation and/or sublimation procedures, temperatures, and times identical with those described for the syntheses of *commo*-silabis(carborane) and *closo*-germacarborane derivatives,[24-26] the off-white residue gave the corresponding *closo*-gallacarborane derivative as a thick syrupy liquid that turned into a crystalline solid when cooled to −78 °C in the detachable U-trap. After careful fractionation of the products, *closo*-1-(*t*-C_4H_9)-1-Ga-2,3-$(SiMe_3)_2$-2,3-$C_2B_4H_4$ (I) (2.32 g, 6.98 mmol; collected at 25 °C; 73% yield), *closo*-1-(*t*-C_4H_9)-1-Ga-2-$(SiMe_3)$-3-(Me)-2,3-$C_2B_4H_4$ (II) (2.36 g, 8.24 mmol; collected at 0 °C; 83% yield), or *closo*-1-(*t*-C_4H_9)-1-Ga-2-$(SiMe_3)$-2,3-$C_2B_4H_5$ (III) (1.74 g, 6.39 mmol; collected at 0 °C; 62% yield) was isolated in reasonably high purity. The corresponding neutral *nido*-carborane precursor 2-$(SiMe_3)$-3-(Me)-2,3-$C_2B_4H_6$ (0.87 g, 3.96 mmol; 0.22 g, 1.36 mmol; 0.45 g, 3.05 mmol) was recovered in a trap held at −78 °C.

The physical properties and characterization of I are as follows: clear oily liquid at room temperature that crystallizes at 0 °C; bp 135 °C under high vacuum (10^{-4} Torr); sensitive to air and moisture; at 25 °C, highly soluble in both polar and nonpolar organic solvents; ^1H NMR (C_6D_6, relative to external Me_4Si) δ 4.86 [q (br), 2 H, basal H_t, $^1J(^1H-^{11}B)$ = 144 Hz], 4.26 [q (br), 1 H, basal H_t, $^1J(^1H-^{11}B)$ = 130 Hz], 0.72 [s, 3 H, *t*-Bu Me], 0.70 [s, 6 H, *t*-Bu Me], 0.35 [s, 18 H, $SiMe_3$], 0.50 [q (br), 1 H, apical H_t, $^1J(^1H-^{11}B)$ = 173 Hz]; ^{11}B NMR (C_6D_6, relative to external $BF_3{\cdot}OEt_2$) δ 17.50 [d, 2 B, basal BH, $^1J(^{11}B-^1H)$ = 143.3 Hz], 10.16 [d, 1 B, basal BH, $^1J(^{11}B-^1H)$ = 129.4 Hz], −37.31 [d, 1 B, apical BH, $^1J(^{11}B-^1H)$ = 172.8 Hz]; ^{13}C NMR (C_6D_6, relative to external Me_4Si) δ 126.00 [s (br), cage carbons (SiCB)], 30.21 [s (br), *t*-Bu $(Me)_3C$], 29.91 [q of m, *t*-Bu Me, $^1J(^{13}C-^1H)$ = 125.8 Hz, $^3J(^{13}C-^1H)$ = 5.6 Hz], 2.52 [q, $SiMe_3$, $^1J(^{13}C-^1H)$ = 120.9 Hz]; mass spectral analysis (high-resolution electron impact (HREI) peak match): theoretical mass for $^{12}C_{12}{}^1H_{31}{}^{10}B_2{}^{11}B_2{}^{28}Si_2{}^{69}Ga$, $^{12}C_{12}{}^1H_{31}{}^{10}B^{11}B_3{}^{28}Si_2{}^{69}Ga$, and $^{12}C_{12}{}^1H_{31}{}^{11}B_4{}^{28}Si_2{}^{69}Ga$ *m/e* 342.1665, 343.1629, and 344.1592; measured mass *m/e* 342.1660, 343.1628, and 344.1607. The details of the IR and mass spectral data for I, together with their assignments, are summarized in Supplementary Tables 1 and 2.

The physical properties and characterization of II are as follows: clear oily liquid at room temperature that crystallizes at 0 °C; bp 148 °C under high vacuum (10^{-4} Torr); sensitive to air and moisture; at 25 °C, highly soluble in both polar and nonpolar organic solvents; ^1H NMR (C_6D_6, relative to external Me_4Si) δ 4.10 [q (br), 2 H, basal H_t, $^1J(^1H-^{11}B)$ = 149 Hz], 3.86 [q (br), 1 H, basal H_t, $^1J(^1H-^{11}B)$ = 143 Hz], 2.50 [s, 3 H, C_{cage}–Me], 0.97 [s, 9 H, *t*-Bu Me], 0.29 [s, 9 H, $SiMe_3$], −0.45 [q (br), 1 H, apical H_t, $^1J(^1H-^{11}B)$ = 175 Hz]; ^{11}B NMR (C_6D_6, relative to external $BF_3{\cdot}OEt_2$) δ 12.22 [d, 2 B, basal BH, $^1J(^{11}B-^1H)$ = 148.6 Hz], 6.34 [d, 1 B, basal BH, $^1J(^{11}B-^1H)$ = 142.7 Hz], −36.23 [d, 1 B, apical BH, $^1J(^{11}B-^1H)$ = 175.5 Hz]; ^{13}C NMR (C_6D_6, relative to external Me_4Si) δ 127.00 [s (br), cage carbon (SiCB)], 122.11 [s (br), cage

---

(16) Grimes, R. N.; Rademaker, W. J.; Denniston, M. L.; Bryan, R. F.; Greene, P. T. *J. Am. Chem. Soc.* **1972**, *94*, 1865.

(17) Bandman, M. A.; Knobler, C. B.; Hawthorne, M. F. *Inorg. Chem.* **1989**, *28*, 1204.

(18) Hosmane, N. S.; Sirmokadam, N. N.; Mollenhauer, M. N. *J. Organomet. Chem.* **1985**, *279*, 359.

(19) Hosmane, N. S.; Mollenhauer, M. N.; Cowley, A. H.; Norman, N. C. *Organometallics* **1985**, *4*, 1194.

(20) Hosmane, N. S.; Maldar, N. N.; Potts, S. B.; Rankin, D. W. H.; Robertson, H. E. *Inorg. Chem.* **1986**, *25*, 1561.

(21) Hosmane, N. S.; Islam, M. S.; Burns, E. G. *Inorg. Chem.* **1987**, *26*, 3236.

(22) The monoanion actually exists as the $(C_4H_8O{\cdot}Na^+)_2$[2-$(SiMe_3)$-3-(R)-2,3-$C_2B_4H_5^-]_2$ dimer (see Scheme I); for preparation and structure see: Hosmane, N. S.; Siriwardane, U.; Zhang, G.; Zhu, H.; Maguire, J. A. *J. Chem. Soc., Chem. Commun.* **1989**, 1128 and references therein.

(23) Cleaver, W. M.; Barron, A. R. *Chemtronics* **1989**, *4*, 146.

(24) Hosmane, N. S.; de Meester, P.; Siriwardane, U.; Islam, M. S.; Chu, S. S. C. *J. Chem. Soc., Chem. Commun.* **1986**, 1421.

(25) Siriwardane, U.; Islam, M. S.; West, T. A.; Hosmane, N. S.; Maguire, J. A.; Cowley, A. H. *J. Am. Chem. Soc.* **1987**, *109*, 4600.

(26) Hosmane, N. S.; Islam, M. S.; Pinkston, B. S.; Siriwardane, U.; Banewicz, J. J.; Maguire, J. A. *Organometallics* **1988**, *7*, 2340.

carbon (CCB)], 31.62 [s (br), *t*-Bu (Me)$_3$C], 30.77 [q of m, *t*-Bu Me, $^{1}J(^{13}C-^{1}H)$ = 125.76 Hz, $^{3}J(^{13}C-^{1}H)$ = 5.54 Hz], 22.73 [q, C$_{cage}$–Me, $^{1}J(^{13}C-^{1}H)$ = 124.13 Hz], 1.99 [q, SiMe$_3$, $^{1}J(^{13}C-^{1}H)$ = 121.6 Hz]. Mass spectral analysis (high-resolution electron impact (HREI) peak match): theoretical mass for $^{12}C_{10}{}^{1}H_{25}{}^{10}B_2{}^{11}B_2{}^{28}Si^{69}Ga$, $^{12}C_{10}{}^{1}H_{25}{}^{10}B^{11}B_3{}^{28}Si^{69}Ga$, and $^{12}C_{10}{}^{1}H_{25}{}^{11}B_4{}^{28}Si^{69}Ga$ *m/e* 284.1426, 285.1390, and 286.1353; measured mass *m/e* 284.1421. 285.1390, and 286.1369. The details of the IR and mass spectral data for II, together with their assignments, are summarized in Supplementary Tables 1 and 2.

The physical properties and characterization of III are as follows: clear oily liquid; bp 127 °C under high vacuum (10^{-4} Torr); sensitive to air and moisture; at 25 °C, highly soluble in both polar and nonpolar organic solvents; ^{1}H NMR (C$_6$D$_6$, relative to external Me$_4$Si) δ 6.59 [s (br), 1 H, cage CH], 3.81 [q (br), 2 H, basal H$_t$, $^{1}J(^{1}H-^{11}B)$ = 138 Hz], 3.30 [q (br), 1 H, basal H$_t$, $^{1}J(^{1}H-^{11}B)$ = 136 Hz], 0.94 [s, 9 H, *t*-Bu Me], 0.23 [s, 9 H, SiMe$_3$], –0.11 [q (br), 1 H, apical H$_t$, $^{1}J(^{1}H-^{11}B)$ = 173 Hz]; ^{11}B NMR (C$_6$D$_6$, relative to external BF$_3$·OEt$_2$) δ 11.46 [d, 2 B, basal BH, $^{1}J(^{11}B-^{1}H)$ = 137.2 Hz], 6.68 [d, 1 B, basal BH, $^{1}J(^{11}B-^{1}H)$ = 136.2 Hz], –39.68 [d, 1 B, apical BH, $^{1}J(^{11}B-^{1}H)$ = 172.5 Hz]; ^{13}C NMR (C$_6$D$_6$, relative to external Me$_4$Si) δ 121.00 [s (br), cage carbon (SiCB)], 110.78 [d (br), cage CH, $^{1}J(^{13}C-^{1}H)$ = 177.25 Hz], 30.07 [s (br), *t*-Bu (Me)$_3$C], 29.41 [q of m, *t*-Bu Me, $^{1}J(^{13}C-^{1}H)$ = 125.14 Hz, $^{3}J(^{13}C-^{1}H)$ = 5.6 Hz], –0.61 [q, SiMe$_3$, $^{1}J(^{13}C-^{1}H)$ = 118.93 Hz]. Mass spectral analysis (high-resolution electron impact (HREI) peak match): theoretical mass for $^{12}C_9{}^{1}H_{23}{}^{10}B_3{}^{11}B^{28}Si^{69}Ga$, $^{12}C_9{}^{1}H_{23}{}^{10}B_2{}^{11}B_2{}^{28}Si^{69}Ga$, and $^{12}C_9{}^{1}H_{23}{}^{10}B^{11}B_3{}^{28}Si^{69}Ga$ *m/e* 269.1306, 270.1270, and 271.1233; measured mass *m/e* 269.1307, 270.1272, and 271.1239. The details of the IR and mass spectral data for III, together with their assignments, are summarized in Supplementary Tables 1 and 2.

Synthesis of 1,1′-(2,2′-C$_8$H$_6$N$_4$)[1-(*t*-C$_4$H$_9$)-1-Ga-2-(SiMe$_3$)-3-(R)-2,3-C$_2$B$_4$H$_4$]$_2$ (R = SiMe$_3$, Me, H). In a procedure identical with that employed for the synthesis of donor–acceptor complexes involving 2,2′-bipyrimidine and *closo*-stanna- or *closo*-plumbacarboranes, described elsewhere,[27-29] 3.84 mmol (1.32 g) of *closo*-1-(*t*-C$_4$H$_9$)-1-Ga-2,3-(SiMe$_3$)$_2$-2,3-C$_2$B$_4$H$_4$ (I), 3.91 mmol (1.12 g) of *closo*-1-(*t*-C$_4$H$_9$)-1-Ga-2-(SiMe$_3$)-3-(Me)-2,3-C$_2$B$_4$H$_4$ (II), or 3.60 mmol (0.98 g) of *closo*-1-(*t*-C$_4$H$_9$)-1-Ga-2-(SiMe$_3$)-2,3-C$_2$B$_4$H$_5$ (III) was treated with freshly sublimed, anhydrous 2,2′-bipyrimidine, C$_8$H$_6$N$_4$ (0.30 g, 1.92 mmol; 0.31 g, 1.96 mmol; 0.28 g, 1.80 mmol) in dry benzene at room temperature for 1 h. This resulted in the isolation of red crystals of 1,1′-(2,2′-C$_8$H$_6$N$_4$)[1-(*t*-C$_4$H$_9$)-1-Ga-2,3-(SiMe$_3$)$_2$-2,3-C$_2$B$_4$H$_4$]$_2$ (IV; 1.40 g, 1.65 mmol; 86% yield), 1,1′-(2,2′-C$_8$H$_6$N$_4$)[1-(*t*-C$_4$H$_9$)-1-Ga-2-(SiMe$_3$)-3-(Me)-2,3-C$_2$B$_4$H$_4$]$_2$ (V; 1.23 g, 1.68 mmol; 86% yield), or 1,1′-(2,2′-C$_8$H$_6$N$_4$)[1-(*t*-C$_4$H$_9$)-1-Ga-2-(SiMe$_3$)-3-(H)-2,3-C$_2$B$_4$H$_4$]$_2$ (VI; 0.94 g, 1.34 mmol; 74% yield) as the only sublimed reaction product on the inside walls of the detachable U-trap. The side arms of both the reaction flask and the U-trap were maintained at 150–160 °C by means of a heating tape during the sublimation. A trace quantity of unreacted 2,2′-bipyrimidine was also recovered in a trap held at –196 °C during the mild sublimation of the orange reaction residue. The gallacarborane precursors and their decomposition product, elemental gallium (Ga^0), were not identified in the sublimate. A small quantity of a dark brown residue that remained in the reaction flask after sublimation was discarded because of its insolubility in organic solvents. Since the complexes IV–VI have limited solubility in nonpolar organic solvents at room temperature, they were recrystallized from hot benzene.

The physical properties and characterization of IV are as follows: mp 195–196 °C; sensitive to air and moisture; slightly soluble in CDCl$_3$, C$_6$D$_6$, and THF, the solubility increasing at higher temperature without decomposition; ^{1}H NMR (C$_6$D$_6$, relative to external Me$_4$Si) δ 8.36 [d, 2 H, bpmd ring, $^{3}J(^{1}H-^{1}H)$ = 5.53 Hz], 6.11 [t, 1 H, bpmd ring, $^{3}J(^{1}H-^{1}H)$ = 5.53 Hz], 4.82 [q (br), 2 H, basal H$_t$, $^{1}J(^{1}H-^{11}B)$ = ~139 Hz], 4.07 [q (br), 1 H, basal H$_t$, $^{1}J(^{1}H-^{11}B)$ = 135 Hz], 0.66 [s, 9 H, *t*-Bu Me], 0.64 [s, 18 H, SiMe$_3$], –0.36 [q (br), 1 H, apical H$_t$, $^{1}J(^{1}H-^{11}B)$ = 176 Hz]; ^{11}B NMR (C$_6$D$_6$, relative to external BF$_3$·OEt$_2$) δ 17.21 [d (v br), 2 B, basal BH, $^{1}J(^{11}B-^{1}H)$ unresolved], 6.89 [d (br), 1 B, basal BH, $^{1}J(^{11}B-^{1}H)$ = 135 Hz], –42.97 [d (br), 1 B, apical BH, $^{1}J(^{11}B-^{1}H)$ = 176.1 Hz]; ^{13}C NMR (C$_6$D$_6$, relative to external Me$_4$Si) δ 157.22 [d, 2 CH, bpmd ring, $^{1}J(^{13}C-^{1}H)$ = 187.7 Hz], 156.26 [s, 1 C, bpmd ring, NCN], 125.24 [s (br), cage carbons (SiCB)], 122.93 [d, 1 CH, bpmd ring, $^{1}J(^{13}C-^{1}H)$ = 171.9 Hz], 30.91 [q of m, *t*-Bu Me, $^{1}J(^{13}C-^{1}H)$ = 126 Hz, $^{3}J(^{13}C-^{1}H)$ = 5.5 Hz], 30.30 [s (br), *t*-Bu (Me)$_3$C], 3.25 [q (br), SiMe$_3$, $^{1}J(^{13}C-^{1}H)$ = 119.7 Hz]. Mass spectral analysis (high-resolution electron impact (HREI) peak match): theoretical mass for $^{12}C_{32}{}^{1}H_{68}{}^{14}N_4{}^{10}B_4{}^{11}B_4{}^{28}Si_4{}^{69}Ga_2$, $^{12}C_{32}{}^{1}H_{68}{}^{14}N_4{}^{10}B_3{}^{11}B_5{}^{28}Si_4{}^{69}Ga_2$, and $^{12}C_{32}{}^{1}H_{68}{}^{14}N_4{}^{10}B_2{}^{11}B_6{}^{28}Si_4{}^{69}Ga_2$ *m/e* 842.3922, 843.3886, and 844.3849; measured mass *m/e* 842.3858, 843.3821, and 844.3765. The details of the IR and mass spectral data of IV, together with their assignments, are summarized in Supplementary Tables 1 and 2.

The physical properties and characterization of V are as follows: mp 205–206 °C; sensitive to air and moisture; slightly soluble in THF, CDCl$_3$, and C$_6$D$_6$, the solubility increasing at higher temperature without any decomposition; ^{1}H NMR (C$_6$D$_6$, relative to external Me$_4$Si) δ 8.34 [d, 2 H, bpmd ring, $^{3}J(^{1}H-^{1}H)$ = 5.4 Hz], 6.10 [t, 1 H, bpmd ring, $^{3}J(^{1}H-^{1}H)$ = 5.4 Hz], 4.4 [q (br), 2 H, basal H$_t$, $^{1}J(^{1}H-^{11}B)$ = 138 Hz], 3.9 [q (br), 1 H, basal H$_t$, $^{1}J(^{1}H-^{11}B)$ = 140 Hz], 2.84 [s, 3 H, C$_{cage}$–Me], 0.66 [s, 9 H, *t*-Bu Me], 0.63 [s, 9 H, SiMe$_3$], –0.41 [q (br), apical H$_t$, $^{1}J(^{1}H-^{11}B)$ = 174 Hz]; ^{11}B NMR (C$_6$D$_6$, relative to external BF$_3$·OEt$_2$) δ 12.30 [d (br), 2 B, basal BH, $^{1}J(^{11}B-^{1}H)$ = 138 Hz], 4.60 [d (br), 1 B, basal BH, $^{1}J(^{11}B-^{1}H)$ = 140 Hz], –41.89 [d (br), 1 B, apical BH, $^{1}J(^{11}B-^{1}H)$ = 174.38 Hz]; ^{13}C NMR (C$_6$D$_6$, relative to external Me$_4$Si) δ 157.64 [d, 2 CH, bpmd ring, $^{1}J(^{13}C-^{1}H)$ = 188 Hz], 155.79 [s, 1 C, bpmd ring, NCN], 125.3 [s (br), cage carbon (SiCB)], 122.41 [d, 1 CH, bpmd ring, $^{1}J(^{13}C-^{1}H)$ = 172 Hz], 120.32 [s (br), cage carbon (CCB)], 31.28 [q of m, *t*-Bu Me, $^{1}J(^{13}C-^{1}H)$ = 125.69 Hz, $^{3}J(^{13}C-^{1}H)$ = 5.4 Hz], 30.68 [s (br), *t*-Bu (Me)$_3$C], 23.03 [q, 1 C, C$_{cage}$–Me, $^{1}J(^{13}C-^{1}H)$ = 124 Hz], 2.24 [q, 3 C, SiMe$_3$, $^{1}J(^{13}C-^{1}H)$ = 119 Hz]. The IR spectral data of V are summarized in Supplementary Table 1.

The physical properties and characterization of VI are as follows: mp 186–187 °C; sensitive to air and moisture; slightly soluble in C$_6$D$_6$, THF, and CDCl$_3$, the solubility increasing at higher temperature without any decomposition; ^{1}H NMR (C$_6$D$_6$, relative to external Me$_4$Si) δ 8.39 [d, 2 H, bpmd ring, $^{3}J(^{1}H-^{1}H)$ = 5.93 Hz], 6.80 [s (br), 1 H, cage CH], 6.25 [t, 1 H, bpmd ring, $^{3}J(^{1}H-^{1}H)$ = 5.96 Hz], 3.79 [q (br), 2 H, basal H$_t$, $^{1}J(^{1}H-^{11}B)$ = 137 Hz], 3.21 [q (br), 1 H, basal H$_t$, $^{1}J(^{1}H-^{11}B)$ = 135 Hz], 0.68 [s, 9 H, *t*-Bu Me], 0.65 [s, 9 H, SiMe$_3$], –0.18 [q (br), 1 H, apical H$_t$, $^{1}J(^{1}H-^{11}B)$ = 172 Hz]; ^{11}B NMR (C$_6$D$_6$, relative to external BF$_3$·OEt$_2$) δ 10.56 [d (br), 2 B, basal BH, $^{1}J(^{11}B-^{1}H)$ = 136.62 Hz], 6.29 [d (br), 1 B, basal BH, $^{1}J(^{11}B-^{1}H)$ = 135 Hz], –47.59 [d (br), 1 B, apical BH, $^{1}J(^{11}B-^{1}H)$ = 172.5 Hz]; ^{13}C NMR (C$_6$D$_6$, relative to external Me$_4$Si) δ 157.30 [d, 2 CH, bpmd ring, $^{1}J(^{13}C-^{1}H)$ = 186 Hz], 156.75 [s, 1 C, bpmd ring, NCN], 122.73 [d, 1 CH, bpmd ring, $^{1}J(^{13}C-^{1}H)$ = 171 Hz], 120.01 [s (br), 1 C, cage carbon (SiCB)], 113.02 [d, C$_{cage}$–H, $^{1}J(^{13}C-^{1}H)$ = 177 Hz], 31.41 [q of m, *t*-Bu Me, $^{1}J(^{13}C-^{1}H)$ = 126 Hz, $^{3}J(^{13}C-^{1}H)$ = 5.6 Hz], 30.88 [s (br), *t*-Bu (Me)$_3$C], 0.54 [q, 3 C, SiMe$_3$, $^{1}J(^{13}C-^{1}H)$ = 119 Hz]. The IR spectral data of VI are summarized in Supplementary Table 1.

X-ray Analyses of *closo*-1-(*t*-C$_4$H$_9$)-1-Ga-2,3-(SiMe$_3$)$_2$-2,3-C$_2$B$_4$H$_4$ (I) and 1,1′-(2,2′-C$_8$H$_6$N$_4$)-[1-(*t*-C$_4$H$_9$)-1-Ga-2,3-(SiMe$_3$)$_2$-2,3-C$_2$B$_4$H$_4$]$_2$ (IV). Transparent hexagonal crystals of I were grown over a period of days from its colorless oily liquid in vacuum-sealed glass tubes held at 0 °C. Bright red crystals of IV were grown in vacuo from benzene solution. Since the crystals of I melt at room temperatures, and the crystals of IV are sensitive to air and/or moisture, both samples were introduced quickly into 0.5-mm Lindemann glass capillaries in a drybox, sealed with an epoxy resin, and mounted rapidly on an automatic Nicolet R3m/V diffractometer. The data were collected with Mo Kα radiation at 230 K. Unit-cell dimensions were refined by a least-squares fit of 24 accurately centered reflections measured in the ranges 18° < 2θ < 25° and 15° < 2θ < 25° for I and IV, respectively. The pertinent crystallographic data are summarized in Table I. Three standard reflections were remeasured after every 100 reflections during the data collection. These data were corrected for decay, Lorentz–polarization effects, and absorption

---

(27) Hosmane, N. S.; Islam, M. S.; Siriwardane, U.; Maguire, J. A.; Campana, C. F. *Organometallics* **1987**, *6*, 2447.

(28) Hosmane, N. S.; Fagner, J. S.; Zhu, H.; Siriwardane, U.; Maguire, J. A.; Zhang, G.; Pinkston, B. S. *Organometallics* **1989**, *8*, 1769.

(29) Hosmane, N. S.; Lu, K.-J.; Siriwardane, U.; Shet, M. S. *Organometallics* **1990**, *9*, 2798.

Table I. Crystallographic Data[a] for I and IV

	I	IV
formula	$C_{12}H_{31}B_4Si_2Ga$	$C_{32}H_{68}B_8N_4Si_4Ga_2$
fw	344.51	847.18
cryst syst	triclinic	monoclinic
space group	$P\bar{1}$	$C2/c$
a, Å	9.160 (2)	24.732 (10)
b, Å	9.763 (3)	14.190 (4)
c, Å	12.961 (4)	15.797 (5)
α, deg	96.84 (2)	
β, deg	106.56 (2)	117.97 (3)
γ, deg	111.20 (2)	
V, Å^3	1003.3 (5)	4896 (2)
Z	2	4
D_{calcd}, g cm^{-3}	1.14	1.15
cryst dimens, mm	0.25 × 0.20 × 0.30	0.10 × 0.25 × 0.15
scan type	$\theta/2\theta$	$\theta/2\theta$
scan speed in ω: min, max, deg min^{-1}	3.0, 15.0	3.0, 15.0
2θ range, deg	3.0–50.0	3.0–46.0
no. of data collected	3791	3504
T, K	230	230
decay, %	0	0
no. of obsd rflns, $I > 3.0\sigma(I)$	2719	1581
no. of params varied	186	265
GOF	3.40	2.24
R^b	0.047	0.051
$R_w{}^b$	0.063	0.061
$\Delta\rho_{max,min}$, e/Å^3	0.64, −0.36	0.68, −0.48
k^c	0.000 08	0.000 72

[a] Graphite-monochromatized Mo Kα radiation, λ = 0.710 73 Å. [b] $R = \sum||F_o| - |F_c||/\sum|F_o|$; $R_w = [\sum_w(F_o - F_c)^2/\sum_w(F_o)^2]^{1/2}$. [c] $w = 1/[\sigma^2(F_o) + k(F_o)^2]$.

(on the basis of ψ scans). The structures were solved by SHELXTL-PLUS[30] and subsequent difference Fourier maps. The cage hydrogen atoms of I were located in difference Fourier maps, and their positions were refined. However, the silylmethyl and *tert*-butyl hydrogen atoms were placed in calculated positions and were included in the refinement with fixed isotropic thermal parameters. Final full-matrix least-squares refinements were carried out with use of the SHELXTL-PLUS system of programs.[30] Neutral-atom scattering factors were taken from ref 31. The function minimized was $\sum w(|F_o| - |F_c|)^2$. All non-hydrogen atoms of I and IV were refined anisotropically. However, the carbon atoms of the trimethylsilyl and *tert*-butyl moieties in IV were disordered. The final refinement of these atoms revealed occupancies of approximately 60% and 40% of the "majority" and "minority" (labeled with a prime (′)) atoms, respectively. In the final stages of refinement a weighting scheme was used (see Table I). The final atomic coordinates are listed in Table II. Selected bond lengths and bond angles are presented in Table III. Selected torsion angles for I, and the mean deviations and dihedral angles of the least-squares planes in IV, are given in Table IV.

Table II. Atomic Coordinates (×10^4) and Equivalent Isotropic Displacement Parameters (Å^2 × 10^3) for I and IV

	x	y	z	U(eq)[a]
		Compound I		
Ga	1273 (1)	4547 (1)	1719 (1)	40 (1)
Si(1)	−33 (2)	1289 (2)	3230 (1)	40 (1)
Si(2)	−3263 (2)	2837 (2)	1762 (1)	39 (1)
C(1)	−102 (6)	2273 (5)	2062 (4)	28 (2)
C(2)	−1347 (6)	2835 (6)	1484 (4)	31 (2)
B(3)	−1113 (8)	3225 (8)	381 (6)	38 (3)
B(4)	476 (10)	2788 (9)	273 (6)	47 (3)
B(5)	1111 (9)	2223 (8)	1419 (6)	46 (3)
B(6)	−1040 (9)	1530 (8)	649 (5)	39 (3)
C(7)	2723 (7)	6391 (6)	2931 (5)	40 (3)
C(8)	2887 (9)	5985 (8)	4038 (5)	70 (4)
C(9)	4425 (8)	7019 (7)	2820 (6)	67 (4)
C(10)	2037 (10)	7588 (7)	2872 (6)	73 (4)
C(11)	−1323 (8)	−774 (6)	2633 (6)	56 (3)
C(12)	2157 (8)	1586 (8)	3973 (6)	66 (4)
C(13)	−689 (10)	2024 (8)	4327 (5)	66 (4)
C(14)	−4591 (8)	3253 (9)	574 (6)	73 (4)
C(15)	−4523 (8)	976 (7)	1911 (6)	57 (3)
C(16)	−2594 (9)	4371 (7)	3013 (6)	63 (4)
		Compound IV		
Ga	4291 (1)	3148 (1)	4216 (1)	52 (1)
Si(1)	3583 (2)	872 (2)	1955 (3)	91 (2)
Si(2)	2502 (1)	1703 (2)	2954 (2)	72 (2)
C(1)	3612 (4)	1980 (6)	2637 (6)	45 (4)
C(2)	3179 (4)	2321 (6)	2973 (6)	43 (4)
B(3)	3259 (5)	3400 (7)	3221 (7)	46 (5)
B(4)	3793 (5)	3802 (7)	2910 (8)	56 (6)
B(5)	4044 (5)	2753 (8)	2637 (7)	50 (5)
B(6)	3245 (5)	3016 (7)	2146 (8)	51 (5)
C(7)	4623 (5)	2233 (7)	5291 (7)	78 (6)
C(8)[b]	5209 (7)	2566 (14)	6098 (11)	68 (10)
C(9)	4141 (8)	2149 (15)	5705 (13)	117 (13)
C(10)	4654 (11)	1262 (11)	4966 (12)	102 (15)
C(8′)	4977 (14)	2621 (25)	6268 (20)	76 (13)
C(9′)	4240 (13)	1420 (22)	5191 (24)	96 (12)
C(10′)	5190 (13)	1687 (21)	5087 (20)	88 (10)
C(11)	2772 (7)	547 (13)	1065 (10)	92 (12)
C(12)	3875 (8)	1132 (11)	1013 (12)	93 (13)
C(13)	4015 (8)	−97 (10)	2644 (11)	87 (12)
C(11′)	3397 (13)	−208 (18)	2632 (20)	106 (11)
C(12′)	3079 (14)	670 (29)	777 (16)	152 (18)
C(13′)	4410 (9)	475 (23)	2428 (21)	110 (11)
C(14)	2409 (9)	2232 (17)	3953 (13)	150 (19)
C(15)	1817 (7)	1783 (18)	1829 (11)	129 (15)
C(16)	2745 (8)	435 (9)	3369 (11)	85 (11)
C(14′)	1934 (11)	2617 (17)	3064 (19)	79 (8)
C(15′)	1974 (15)	1232 (20)	1702 (18)	74 (12)
C(16′)	2580 (14)	798 (20)	3840 (20)	97 (12)
N(1)	4350 (3)	4516 (5)	5073 (5)	49 (4)
N(2)	5168 (3)	3976 (5)	4494 (5)	56 (4)
C(17)	4770 (3)	5144 (6)	5170 (6)	41 (4)
C(18)	5568 (5)	3729 (8)	4182 (7)	71 (6)
C(19)	6030 (4)	4316 (8)	4267 (7)	71 (6)
C(20)	3942 (4)	4799 (7)	5350 (7)	60 (5)

[a] Equivalent isotropic U, defined as one-third of the trace of the orthogonalized U_{ij} tensor. [b] Atoms C(8), C(9), ..., C(16) represent 60% occupancy, while the atoms labeled with primes (′) possess 40% occupancy.

Results and Discussion

Synthesis. The reaction of $[Ga(t\text{-}C_4H_9)Cl_2]_2$ with the *nido*-carborane dianionic double salts $Na^+Li^+[2\text{-}(SiMe_3)\text{-}3\text{-}(R)\text{-}2,3\text{-}C_2B_4H_4]^{2-}$ (R = SiMe$_3$, Me, H) in a molar ratio of 1:2 in THF solution produced *closo*-1-(t-C_4H_9)-1-Ga-2,3-$(SiMe_3)_2$-2,3-$C_2B_4H_4$ (I), *closo*-1-(t-C_4H_9)-1-Ga-2-($SiMe_3$)-3-(Me)-2,3-$C_2B_4H_4$ (II), and *closo*-1-(t-C_4H_9)-1-Ga-2-($SiMe_3$)-2,3-$C_2B_4H_5$ (III) as moderately air-sensitive colorless oily liquids, in 71, 83, and 62% yields, respectively (Scheme I). The only previous compound of this type, *closo*-1-methyl-1-galla-2,3-dicarbaheptaborane, was synthesized in 20–30% yields by Grimes et al.[16] by the gas-phase reaction of trimethylgallium with $C_2B_4H_8$. Our method is an improvement for the following reasons: (i) the difficulties of handling a volatile, flammable reaction mixture are avoided, (ii) the carborane cage is not degraded to involatile solids, (iii) volatile byproducts such as BMe_3 are not formed, and (iv) appreciably higher yields are obtained, hence, the method is suitable for scale-up to gram quantities.

The reaction between *closo*-gallacarborane and 2,2′-bipyrimidine in a ratio of 2:1 in benzene was instantaneous and produced the bridged donor–acceptor complexes 1,1′-(2,2′-$C_8H_6N_4$)[1-(t-C_4H_9)-1-Ga-2,3-$(SiMe_3)_2$-2,3-$C_2B_4H_4]_2$ (IV), 1,1′-(2,2′-$C_8H_6N_4$)[1-(t-C_4H_9)-1-Ga-2-($SiMe_3$)-3-(Me)-2,3-$C_2B_4H_4]_2$ (V), and 1,1′-(2,2′-$C_8H_6N_4$)[1-(t-C_4H_9)-1-Ga-2-($SiMe_3$)-2,3-$C_2B_4H_5]_2$ (VI) in

---

(30) Sheldrick, G. M. *Structure Determination Software Programs*; Nicolet Instrument Corp.: Madison, WI, 1988.

(31) *International Tables for X-ray Crystallography*; Kynoch Press: Birmingham, U.K., 1974; Vol. IV.

Table III. Bond Lengths (Å) and Bond Angles (deg) for I and IV

Bond Lengths							
Compound I							
Ga–Cnt[a]	1.748	Ga–C(1)	2.291 (5)	B(4)–B(6)	1.723 (11)	B(5)–B(6)	1.758 (9)
Ga–C(2)	2.282 (5)	Ga–B(3)	2.171 (5)	C(7)–C(8)	1.515 (10)	C(7)–C9)	1.511 (10)
Ga–B(4)	2.131 (7)	Ga–B(5)	2.199 (8)	C(7)–C(10)	1.515 (11)	Si(1)–C(1)	1.885 (6)
Ga–C(7)	1.970 (5)	B(6)–Cnt	1.076	Si(1)–C(11)	1.854 (5)	Si(1)–C(12)	1.848 (7)
C(1)–C(2)	1.492 (8)	C(1)–B(5)	1.578 (11)	Si(1)–C(13)	1.859 (9)	Si(2)–C(2)	1.890 (7)
C(1)–B(6)	1.719 (8)	C(2)–B(3)	1.576 (10)	Si(2)–C(14)	1.859 (8)	Si(2)–C(15)	1.834 (7)
C(2)–B(6)	1.726 (10)	B(3)–B(4)	1.694 (13)	Si(2)–C(16)	1.855 (7)		
B(3)–B(6)	1.752 (11)	B(4)–B(5)	1.668 (12)				
Compound IV							
Ga–Cnt	2.067	Ga–C(1)	2.804 (10)	C(1)–B(6)	1.710 (12)	C(2)–B(3)	1.570 (13)
Ga–C(2)	2.781 (10)	Ga–B(3)	2.314 (10)	C(2)–B(6)	1.706 (16)	B(3)–B(4)	1.709 (20)
Ga–B(4)	2.062 (11)	Ga–B(5)	2.341 (12)	B(3)–B(6)	1.768 (17)	B(4)–B(5)	1.743 (16)
Ga–C(7)	1.984 (10)	Ga–N(1)	2.332 (8)	B(4)–B(6)	1.732 (13)	B(5)–B(6)	1.791 (15)
Ga–N(2)	2.321 (8)	B(6)–Cnt	1.082	C(7)–C(8)	1.490 (16)	C(7)–C(9)	1.610 (27)
Si(1)–C(1)	1.889 (9)	Si(1)–C(11)	1.889 (13)	C(7)–C(10)	1.485 (20)	C(7)–C(8′)	1.479 (30)
Si(1)–C(12)	1.971 (23)	Si(1)–C(13)	1.767 (15)	C(7)–C(9′)	1.452 (34)	C(7)–C(10′)	1.760 (38)
Si(1)–C(11′)	2.041 (32)	Si(1)–C(12′)	1.710 (22)	N(1)–C(17)	1.321 (12)	N(1)–C(20)	1.336 (16)
Si(1)–C(13′)	1.903 (23)	Si(2)–C(2)	1.877 (10)	N(2)–C(18)	1.342 (17)	N(2)–C(17A)	1.338 (11)
Si(2)–C(14)	1.858 (24)	Si(2)–C(15)	1.794 (13)	C(17)–N(2A)	1.338 (11)	C(17)–C(17A)	1.525 (21)
Si(2)–C(16)	1.912 (13)	Si(2)–C(14′)	1.980 (29)	C(18)–C(19)	1.368 (16)	C(19)–C(20A)	1.380 (15)
Si(2)–C(15′)	1.908 (24)	Si(2)–C(16′)	1.842 (32)	C(20)–C(19A)	1.380 (15)		
C(1)–C(2)	1.480 (15)	C(1)–B(5)	1.532 (15)				
Bond Angles							
Compound I							
Ga–Cnt–B(6)	**171.2**	**C(7)–Ga–Cnt**	**155.8**	C(11)–Si(1)–C(13)	110.6 (3)	C(12)–Si(1)–C(13)	105.8 (3)
C(1)–C(2)–B(3)	**111.4 (6)**	**C(2)–B(3)–B(4)**	**105.6 (6)**	C(2)–Si(2)–C(14)	109.6 (3)	C(2)–Si(2)–C(15)	110.8 (3)
B(3)–B(4)–B(5)	**104.9 (6)**	**C(1)–B(5)–B(4)**	**105.7 (6)**	C(14–Si(2)–C(15)	107.8 (3)	C(2)–Si(2)–C(16)	109.1 (3)
Ga–C(7)–C(8)	**109.4 (4)**	**Ga–C(7)–C(9)**	**107.8 (4)**	C(14)–Si(2)–C(16)	107.5 (4)	C(15)–Si(2)–C(16)	112.0 (3)
Ga–C(7)–C(10)	111.7 (4)	C(8)–C(7)–C(9)	109.6 (5)	Si(1)–C(1)–C(2)	130.4 (4)	Si(1)–C(1)–B(5)	116.1 (5)
C(8)–C(7)–C(10)	109.5 (6)	C(9)–C(7)–C(10)	108.8 (5)	C(2)–C(1)–B(5)	112.3 (5)	Si(2)–C(2)–C(1)	129.7 (4)
C(1)–Si(1)–C(11)	108.7 (3)	C(1)–Si(1)–C(12)	108.4 (3)	Si(2)–C(2)–B(3)	118.1 (4)		
C(11)–Si(1)–C(12)	108.4 (3)	C(1)–Si(1)–C(13)	114.8 (3)				
Compound IV							
Ga–Cnt–B(6)	154.8	C(7)–Ga–Cnt	123.7	Si(2)–C(2)–C(1)	129.1 (6)	Si(2)–C(2)–B(3)	117.8 (8)
N(1)–Ga–Cnt	123.7	N(2)–Ga–Cnt	124.8	C(1)–C(2)–B(3)	112.4 (8)	Si(2)–C(2)–B(6)	131.5 (5)
C(7)–Ga–N(1)	99.2 (4)	C(7)–Ga–N(2)	101.3 (4)	C(2)–B(3)–B(4)	106.1 (9)	B(3)–B(4)–B(5)	101.5 (8)
C(1)–Si(1)–C(11)	111.7 (6)	C(1)–Si(1)–C(12)	110.2 (6)	C(1)–B(5)–B(4)	106.3 (10)	Ga–C(7)–C(8)	111.8 (10)
C(11)–Si(1)–C(12)	96.9 (7)	C(1)–Si(1)–C(13)	116.5 (6)	Ga–C(7)–C(9)	108.0 (8)	C(8)–C(7)–C(9)	106.5 (12)
C(11)–Si(1)–C(13)	113.1 (8)	C(12)–Si(1)–C(13)	106.3 (9)	Ga–C(7)–C(10)	112.3 (9)	C(8)–C(7)–C(10)	113.7 (13)
C(1)–Si(1)–C(11′)	106.5 (10)	C(1)–Si(1)–C(12′)	125.0 (14)	C(9)–C(7)–C(10)	103.9 (15)	Ga–C(7)–C(8′)	117.0 (15)
C(11′)–Si(1)–C(12′)	102.4 (15)	C(1)–Si(1)–C(13′)	106.1 (10)	Ga–C(7)–C(9′)	116.1 (12)	C(8′)–C(7)–C(9′)	116.5 (22)
C(11′)–Si(1)–C(13′)	92.1 (13)	C(12′)–Si(1)–C(13′)	118.6 (16)	Ga–C(7)–C(10′)	100.2 (12)	C(8′)–C(7)–C(10′)	102.8 (17)
C(2)–Si(2)–C(14)	105.2 (8)	C(2)–Si(2)–C(15)	114.0 (8)	C(9′)–C(7)–C(10′)	99.5 (18)	Ga–N(1)–C(17)	117.3 (7)
C(14)–Si(2)–C(15)	112.3 (9)	C(2)–Si(2)–C(16)	107.4 (7)	Ga–N(1)–C(20)	126.1 (6)	C(17)–N(1)–C(20)	115.7 (8)
C(14)–Si(2)–C(16)	103.5 (9)	C(15)–Si(2)–C(16)	113.5 (9)	Ga–N(2)–C(18)	125.7 (6)	Ga–N(2)–C(17A)	118.1 (7)
C(2)–Si(2)–C(14′)	110.9 (8)	C(2)–Si(2)–C(15′)	110.6 (12)	C(18)–N(2)–C(17A)	115.0 (9)	N(1)–C(17)–N(2A)	127.8 (10)
C(14′)–Si(2)–C(15′)	98.7 (12)	C(2)–Si(2)–C(16′)	122.6 (10)	N(1)–C(17)–C(17A)	117.1 (9)	N(2A)–C(17)–C(17A)	115.1 (10)
C(14′)–Si(2)–C(16′)	102.5 (15)	C(15′)–Si(2)–C(16′)	108.7 (12)	N(2)–C(18)–C(19)	122.0 (10)	C(18)–C(19)–C(20A)	117.7 (12)
Si(1)–C(1)–C(2)	129.5 (6)	Si(1)–C(1)–B(5)	115.8 (8)	N(1)–C(20)–C(19A)	121.7 (10)		
C(2)–C(1)–B(5)	112.8 (8)	Si(1)–C(1)–B(6)	125.9 (6)				

[a] **Cnt represents the centroid of the C_2B_3 ring.**

74–86% yields. Apparently, the reactivity of the *closo*-gallacarborane toward a Lewis base was enhanced by the Lewis acid nature of the gallium. The somewhat lower yields were due to the formation of nonsublimable and insoluble dark brown residues that remained after sublimation.

Characterization. The *closo*-gallacarboranes I–III and their donor–acceptor complexes IV–VI were characterized on the basis of ^{1}H, ^{11}B, and ^{13}C pulse Fourier transform NMR, IR, and mass spectroscopy (Experimental Section and Supplementary Tables S1 and S2). The complexes I and IV were also characterized by single-crystal X-ray analyses (Tables I–IV). However, the elemental analyses of I–VI gave erroneous results presumably due to their extreme sensitivity toward air and moisture.

Mass Spectra. The low-resolution electron impact mass spectra (LREI) and the isotope patterns of the *closo*-gallacarboranes I–III are consistent with their molecular formulas (see Supplementary Table S2). Although the LREI mass spectrum of IV does not produce the parent ion groupings, the HREI mass spectrum showed an extremely weak parent ion (M^+) grouping. This resulted in rather poor fits between experimental and theoretical values for the exact masses of the molecular species as indicated by the large deviations of about −7.6 to −9.9 ppm (see Experimental Section). Nevertheless, the exact mass measurements unambiguously showed the molecular composition of I–IV.

NMR and IR Spectra. The ^{1}H NMR and ^{13}C NMR spectra indicate the presence of a C_2B_4 carborane cage, *tert*-butyl, SiMe$_3$, and Me or CH groups in compounds I–VI in addition to the presence of a 2,2′-bipyrimidine ligand in each of the donor–acceptor complexes IV–VI. The basal BH proton resonances are significantly shifted downfield from those of the *nido*-carborane precursor in the ^{1}H NMR spectra of I–VI (see Experimental Section). Although these shifts are indicative of deshielding of these protons due to interactions between the apical gallium and

Table IV. Selected Torsion Angles (deg) in Gallacarborane I and Mean Deviations (Å) of Least-Squares Planes and Their Dihedral Angles (deg) Involving the C_2B_3 Face and 2,2′-Bipyrimidine Rings in the Donor–Acceptor Complex IV

Gallacarborane I

atoms	torsion angle
C(7)–Ga–C_2B_3(centroid)–C(1)	−14.4
C(7)–Ga–C_2B_3(centroid)–B(3)	125.9
C(7)–Ga–C_2B_3(centroid)–B(5)	−85.7
C(7)–Ga–C_2B_3(centroid)–C(2)	55.1
C(7)–Ga–C_2B_3(centroid)–B(4)	−159.2

Complex IV

plane	mean dev	plane	mean dev
1 [C_2B_3 ring]	0.042	3 [$C_4N(1)N(2a)$ pmd ring]	0.012
2 [C_8N_4 bipmd ring]	0.013	4 [$C_4N(2)N(1a)$ pmd ring]	0.012

planes	dihedral angle	planes	dihedral angle
1 and 2	11.0	2 and 3	0.1
1 and 3	11.0	2 and 4	0.1
1 and 4	11.0	3 and 4	0

Scheme I

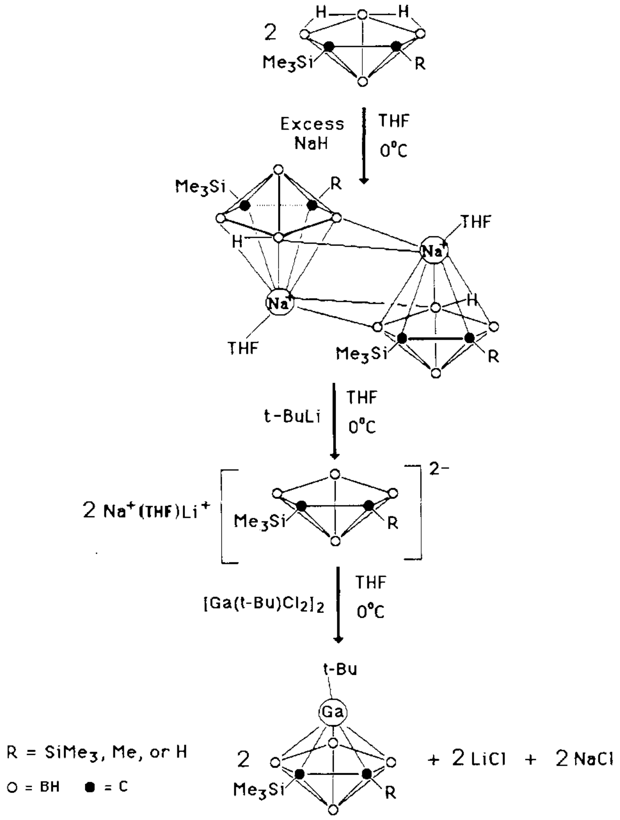

the basal borons, the apical BH proton resonances are shifted less significantly when compared to those of other *closo*-heterocarboranes containing group 14 elements at the apical positions.[25,26,32,33] A similar trend has been observed in their ^{11}B NMR spectra. The apical BH resonances of gallacarboranes I–III (in the region of −36 to −40 ppm) were further shifted upfield by about 6–8 ppm upon coordination to 2,2′-bipyrimidine (see Experimental Section). This trend has been observed previously for all the donor–acceptor complexes of group 14 heterocarboranes.[26-29,33] The significantly upfield shifts of the apical BH resonances of I–III compared with those of the *nido*-carborane precursor are indicative of a weak interaction between the apical gallium and the apical boron through the basal borons and thus imply an extremely slip-distorted closo or, perhaps, cage-opened nido geometries for these compounds. Indeed, the crystal structure of I, discussed in the following section, unambiguously showed a slightly slip-distorted closo geometry similar to that in the corresponding stannacarborane analogue.[11,12] It is conceivable that, unlike the *closo*-stannacarborane system,[32] the *closo*-gallacarboranes exhibit nido geometries in solution.

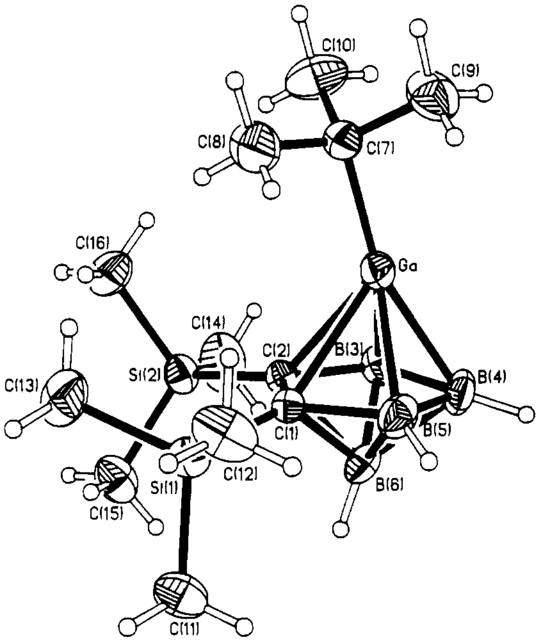

Figure 1. Perspective view of *closo*-1-(*t*-C_4H_9)-1-Ga-2,3-$(SiMe_3)_2$-2,3-$C_2B_4H_4$ (I) showing the atom-numbering scheme. The thermal ellipsoids are drawn at the 40% probability level.

The interesting features in the proton-coupled ^{13}C NMR spectra of I–VI are as follows: (i) the splitting of each line of the quartet due to the nonequivalent methyl protons of the Ga-bound *tert*-butyl group in I–III and (ii) a slightly upfield shift for the NCN carbon of the bipyrimidine ring in each of the complexes IV–VI when compared to those in the free 2,2′-bipyrimidine and its complexes with *closo*-germa-, *closo*-stanna-, and *closo*-plumbacarboranes.[26-29,33,34]

The presence of the gallacarborane cages and the coordinated 2,2′-bipyrimidine was also confirmed by the infrared spectra of I–VI (see Supplementary Table S1). However, the splitting of the B–H stretching mode near 2500 cm^{-1} in the IR spectrum of each of the complexes IV–VI indicates that the location of gallium could be either in a bridging position or in an η^1-bonding posture with respect to the C_2B_4 cage. This feature has been noted for all heteroatom-bridged $C_2B_4H_8$ derivatives.[35] Indeed, the crystal structure of IV (discussed in the following section) confirmed this observation and demonstrates that the complex is severely slip-distorted in such a way that the apical gallium can be viewed as η^1 bonded to the unique boron of the C_2B_3 face.

Crystal Structures of *closo*-1-(*t*-C_4H_9)-1-Ga-2,3-$(SiMe_3)_2$-2,3-$C_2B_4H_4$ (I) and 1,1′-(2,2′-$C_8H_6N_4$)[1-(*t*-

---

[32] Hosmane, N. S.; Sirmokadam, N. N.; Herber, R. H. *Organometallics* **1984**, *3*, 1665.

[33] Hosmane, N. S.; Lu, K.-J.; Zhu, H.; Siriwardane, U.; Shet, M. S.; Maguire, J. A. *Organometallics* **1990**, *9*, 808.

[34] Hosmane, N. S.; de Meester, P.; Maldar, N. N.; Potts, S. B.; Chu, S. S. C.; Herber, R. H. *Organometallics* **1986**, *5*, 772.

[35] Hosmane, N. S.; Grimes, R. N. *Inorg. Chem.* **1979**, *18*, 2886 and references therein.

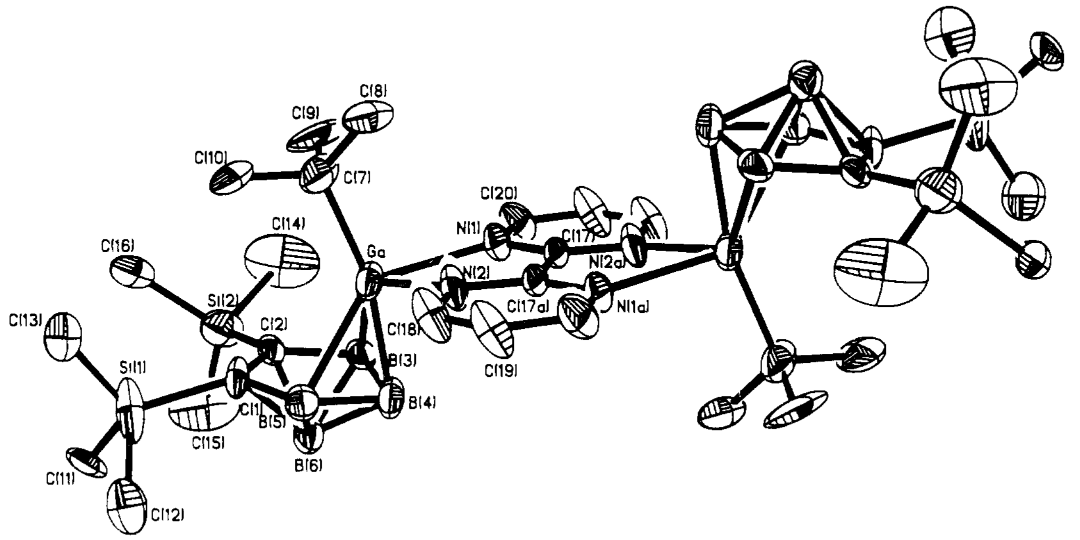

Figure 2. Perspective view of 1,1′-(2,2′-$C_8H_6N_4$)[1-(*t*-C_4H_9)-1-Ga-2,3-$(SiMe_3)_2$-2,3-$C_2B_4H_4$]$_2$ (IV) showing the trans configuration of the gallacarboranes and the atom-numbering scheme. The thermal ellipsoids are drawn at the 40% probability level. The midpoint of the C(17)–C(17a) bond lies at a center of symmetry.

C_4H_9)-1-Ga-2,3-$(SiMe_3)_2$-2,3-$C_2B_4H_4$]$_2$ (IV). The crystal structure of I, shown in Figure 1, is almost identical with that of 1-Me-1-Ga-2,3-$C_2B_4H_6$[15] in that the gallium atom occupies an apical vertex of a pentagonal bipyramid and is slipped significantly toward the unique boron above the C_2B_3 face in an η^3 fashion, thus making the Ga–C_{cage} bonds longer than the Ga–B bonds by about 0.1–0.15 Å (see Table III). The distance from the C_2B_3-centroid to the apical Ga is 1.748 Å, while the distance to the apical boron [B(6)] is 1.076 Å. The Ga-bound *tert*-butyl group is significantly tilted toward the cage carbons above the C_2B_3 face. The angles of tilt of the *tert*-butyl group from the axis that bisects the apical boron and gallium and the axis that bisects the centroid of the C_2B_3 face and the apical gallium are 21 and 24°, respectively. The corresponding angles in 1-Me-1-Ga-2,3-$C_2B_4H_6$[15] are 20 and 23°, respectively. Thus, the slip distortion of the heteroatom and the tilt of the heteroatom-bound moiety, found in the structures of both gallacarboranes, establish a pattern for these systems. Extended Hückel calculations have been employed to explain the reason for the tilt of the Ga-bound methyl moiety in 1-Me-1-Ga-2,3-$C_2B_4H_6$.[36] A similar explanation could be given for the tilt of the Ga-bound *tert*-butyl moiety and the slip distortion in the present case as well. The relative energies of the two occupied molecular orbitals change as the Ga–*tert*-butyl bond is tilted away from the Ga–B_{apex} axis. As the tilt angle increases, the energy of the first MO (4S) drops fairly rapidly while that of the second (2S) increases, but less sharply. The first MO is concentrated mainly on the Ga and the unique boron atoms. Thus, bending increases the overlap between the Ga(*t*-C_4H_9) fragment and the C_2B_4 cage, thereby stabilizing the orbital. The second MO, predominantly a $\pi_{C=C} + \sigma_{Ga(t\text{-}Bu)}$ interaction, is less stabilized upon bending. Since the Ga(*t*-C_4H_9) fragment interacts less significantly with the C_2B_4 cage in the second MO than in the first, there is a net increase in bonding with distortion. Thus, the difference between the extent of fragment interaction in the two molecular orbitals would lead to an overall stabilization upon slippage.

The structure of the adduct IV is illustrated in Figure 2. The distances between the C_2B_3 centroid and the apical Ga and the apical boron atoms are 2.067 and 1.082 Å, respectively, and these are significantly longer than those of its precursor I (see Table III). It is clear that the interactions of both the apical gallium and the apical boron with the C_2B_3 pentagonal face are weakened upon complexation with 2,2′-bipyrimidine. The tilt angles of the Ga-bound *tert*-butyl group from the Ga–B_{apex} and Ga–C_2B_3 centroid axes are 47.7 and 56.3°, respectively, and these values are substantially higher than those in the precursor despite the steric hindrance due to bulky trimethylsilyl groups on the cage carbons. All the distances indicate that the extent of slip distortion in the donor–acceptor complex IV is severe with a difference of about 0.73 Å between the average Ga–C_{cage} and Ga–B_{unique} bonds, thus linking the Ga(*t*-C_4H_9) fragment as an endopolyhedral moiety in an η^1 fashion to the unique boron [B(4)] of the carborane cage (see Figure 2 and Table III). This is an indication of the existence of very strong bonds between the apical Ga and N-donor atoms of the Lewis base in IV [Ga–N(1,2) = 2.325 (8) Å]. It is of interest to note that Hawthorne and coworkers have recently shown the same type of slippage of the apical aluminum and tilt of the Al-bound ethyl group in the structure of the donor–acceptor complex 3,3′-$(Et_3P)_2$-3-(Et)-3-Al-1,2-$C_2B_9H_{11}$.[13] However, the difference between the average M–C_{cage} and M–B_{unique} bonds (M = Sn, Pb) in the 2,2′-bipyrimidine complexes of the *closo*-stannacarboranes and -plumbacarboranes are 0.266 and 0.25–0.28 Å, respectively.[27-29] It has been shown very recently that the most effective bonding between the heteroatom and the Lewis base occurs when the planar bases and the C_2B_3 faces align parallel, that is with a dihedral angle of zero.[37] However, repulsion between the two ligands results in slippage of the apical heteroatom toward the unique boron on complexation with the base by minimizing the interaction of the heteroatom with the cage carbons and reducing the carborane–Lewis base repulsion. In general, when a stronger base interacts with the heteroatom, the slippage of the heteroatom increases and, consequently, the dihedral angles between the base and the C_2B_3 faces decrease. It has been observed in the stannacarborane, germacarborane, and plumbacarborane systems that the adducts with monodentate Lewis bases [(ferrocenylmethyl)dimethylamine] show less slip distor-

---

[36] Canadell, E.; Eisentein, O.; Rubio, J. *Organometallics* **1984**, *3*, 759.

[37] Maguire, J. A.; Ford, G. P.; Hosmane, N. S. *Inorg. Chem.* **1988**, *27*, 3354.

tion than that found in the 2,2′-bipyridine or 1,10-phenanthroline complexes.[26,28,33,34] The observation that the weaker base, 2,2′-bipyrimidine, exhibits a large dihedral angle of about 44° between the C_2B_3 face and the planar Lewis base is consistent with this trend.[27-29] However, the dihedral angle of 11.0° between the two ligands in IV suggests that the interactions between Ga and N-donor atoms are extremely strong and that the the apical Ga is severely slipped toward the unique boron despite the weaker basicity of the 2,2′-bipyrimidine ligand. This is precisely what has been found in the structure of IV. Perhaps, the greater Lewis acidity of the apical gallium is responsible for the unusually strong bonds that exist between the gallacarborane I and 2,2′-bipyrimidine in the donor–acceptor complex IV. As in the cases of the stannacarborane and plumbacarborane systems, the trans orientation of the gallacarboranes in IV is favored on steric grounds.[28,29]

Acknowledgment. This work was supported by grants from the National Science Foundation (CHE-8800328 to N.S.H. and CHE-9005967 to A.H.C.), the Robert A. Welch Foundation (N-1016 to N.S.H. and F-135 to A.H.C.), and the donors of the Petroleum Research Fund, administered by the American Chemical Society (to N.S.H.). The help and assistance of Dr. R. L. Cerny and Mr. C. Jacoby of the Midwest Center for Mass Spectrometry, a National Science Foundation Regional Instrumentation Facility (Grant No. CHE-8211164), are gratefully acknowledged.

Supplementary Material Available: Listings of IR absorptions (Table S-1) and mass spectrometric data (Table S-2) for I–VI and tables of anisotropic displacement coefficients (Table S-3), torsion angles (Table S-4), and H-atom coordinates and isotropic displacement coefficients for I and IV (Table S-5) (10 pages); a listing of structure factors for I and IV (Table S-6) (16 pages). Ordering information is given on any current masthead page.

Synthesis and Reactivity of Neutral and Ionic π-Adducts of Functional Arenes. X-ray Crystal Structures of $\{[(C_5Me_5)Ru]_2(\eta^6,\eta^6\text{-PhC}{\equiv}\text{CPh})\}(CF_3SO_3)_2$, $(C_5Me_5)Ru(\eta^6\text{-PhCOO})$, and $[(C_5Me_5)(MeCN)Ru(\mu_2\text{-}\eta^2,\eta^4\text{-}C_4H_2Ph_2)Ru(C_5Me_5)](CF_3SO_3)$

Xiao Dong He, Bruno Chaudret,* Françoise Dahan, and Yong-Sheng Huang

Laboratoire de Chimie de Coordination du CNRS, UP No. 8241 liée par conventions
à l'Université Paul Sabatier et à l'Institut National Polytechnique, 205 route de Narbonne,
31077 Toulouse Cedex, France

Received June 22, 1990

The protonation of $[Cp^*Ru(OMe)]_2$ (1) in the presence of functional arenes, viz. diphenylacetylene, stilbene, benzophenone, phenol, or benzoic acid, yields the π-arene adducts $[Cp^*Ru(\eta^6\text{-PhC}{\equiv}\text{CPh})](CF_3SO_3)$ (5), $[(Cp^*Ru)_2\ (\eta^6,\eta^6\text{-PhC}{\equiv}\text{CPh})](CF_3SO_3)_2$ (6), $[(Cp^*Ru)_2(\eta^6,\eta^6\text{-PhCH}{=}\text{CHPh})](CF_3SO_3)_2$ (7), $[(Cp^*Ru)_2(\eta^6,\eta^6\text{-PhCOPh})](CF_3SO_3)_2$ (9), $[Cp^*Ru(\eta^6\text{-PhOH})](CF_3SO_3)$ (11), and $[Cp^*Ru(\eta^6\text{-PhCOOH})](CF_3SO_3)$ (14). It is noteworthy that the monoadducts (5) and bis adducts (6) can be obtained with diphenylacetylene, whereas with stilbene and benzophenone the bis adducts (7 and 9) are preferentially obtained under the same conditions. This can be related both to the electron-releasing effect of the "Cp^*Ru^+" fragment and to the better transmission of electronic effects. 1 can be directly protonated by phenol and benzoic acid to yield $[Cp^*Ru(\eta^5\text{-}C_6H_5O)]$ (12) and $[Cp^*Ru(\eta^6\text{-PhCOO})]$ (15). **15** shows a zwitterionic character ascertained by an X-ray crystal structure determination and its reactivity. 12 reacts with CH_3I to give $[Cp^*Ru(\eta^6\text{-PhOCH}_3)]^+$ (13), obtained independently from Cp^*Ru^+ and $PhOCH_3$ but not with a primary amine. Finally, the protonation of $[Cp^*Ru(OMe)]_2$ in the presence of benzonitrile or phenylacetylene leads to untractable mixtures containing both π-aromatic and σ-bonded (PhCN) or more complicated ($PhC{\equiv}CH$) derivatives. However, the reaction of $[Cp^*Ru(MeCN)_3](CF_3SO_3)$ (17) with phenylacetylene affords the paramagnetic complex $[Cp^*(MeCN)Ru(\mu_2\text{-}\eta^2,\eta^4\text{-}C_4H_2Ph_2)RuCp^*](CF_3SO_3)$ (18) in high yield. The structures of **6**, **15**, and **18** have been ascertained by X-ray crystal structure determination.

Introduction

Coordination to a transition metal has been shown to activate aromatic hydrocarbons toward nucleophilic substitution,[1,2] nucleophilic addition, etc.[1,3] Numerous organic syntheses have been carried out in this way for the last 20 years, mainly using the "$Cr(CO)_3$" fragment.[4] It has even been demonstrated lately that catalytic reactions could be assisted by this method.[5]

---

[1] See: Collman, J. P.; Hegedus, L. S.; Norton, J. R.; Finke, R. G. *Principles and Applications of Organotransition Metal Chemistry*; University Science Books: Mill Valley, CA, 1987.

[2] (a) Nicholls, B.; Whiting, M. C. *J. Chem. Soc.* **1959**, 55. (b) Semmelhack, M. F.; Hall, H. T., Jr. *J. Am. Chem. Soc.* **1974**, *96*, 709.

[3] Semmelhack, M. F.; Hall, H. T., Jr.; Farina, R.; Yoshifuji, M.; Clark, G.; Bargar, T.; Hirotsu, K.; Clardy, J. *J. Am. Chem. Soc.* **1979**, *101*, 3535.

[4] See: Davis, R.; Kane-Maguire, L. A. P. In *Comprehensive Organometallic Chemistry*; Wilkinson, G., Stone, F. G. A., Abel, E. W., Eds.; Pergamon Press: Oxford, 1982; Vol. 3, pp 975–1063.

0276-7333/91/2310-0970$02.50/0